Cancer Cell
Article

Regulators of Mitotic Arrest and Ceramide Metabolism Are Determinants of Sensitivity to Paclitaxel and Other Chemotherapeutic Drugs

Charles Swanton,[1,7] Michela Marani,[1,7] Olivier Pardo,[1] Patricia H. Warne,[1] Gavin Kelly,[2] Erik Sahai,[3] Frédéric Elustondo,[4] Jenny Chang,[5] Jillian Temple,[6] Ahmed A. Ahmed,[6] James D. Brenton,[6] Julian Downward,[1,*] and Barbara Nicke[1]

[1] Signal Transduction
[2] Bioinformatics and Biostatistics
[3] Tumour Cell Biology Laboratories
Cancer Research UK London Research Institute, 44 Lincoln's Inn Fields, London WC2A 3PX, UK
[4] Medicinal Chemistry, Cancer Research Technology, Wolfson Institute for Biomedical Research, University College London, London, WC1E 6BT, UK
[5] Breast Center, Baylor College of Medicine, 1 Baylor Plaza MS 600, Houston, TX 77030, USA
[6] Functional Genomics of Drug Resistance Laboratory, Cambridge Research Institute, Cambridge CB2 2XZ, UK
[7] These authors contributed equally to this work.
*Correspondence: julian.downward@cancer.org.uk
DOI 10.1016/j.ccr.2007.04.011

SUMMARY

Cytotoxic drug resistance is a major cause of cancer treatment failure. We report an RNA interference screen to identify genes influencing sensitivity of different cancer cell types to chemotherapeutic agents. A set of genes whose targeting leads to resistance to paclitaxel is identified, many of which are involved in the spindle assembly checkpoint. Silencing these genes attenuates paclitaxel-induced mitotic arrest and induces polyploidy in the absence of drug. We also identify a ceramide transport protein, COL4A3BP or CERT, whose downregulation sensitizes cancer cells to multiple cytotoxic agents, potentiating endoplasmic reticulum stress. COL4A3BP expression is increased in drug-resistant cell lines and in residual tumor following paclitaxel treatment of ovarian cancer, suggesting that it could be a target for chemotherapy-resistant cancers.

INTRODUCTION

Chemotherapeutic drug resistance is a fundamental problem in cancer management, responsible for most cases of treatment failure in patients with metastatic cancer. Tumors can be intrinsically resistant to chemotherapy before treatment or acquire resistance during treatment as a result of microevolutionary pressure on tumor cells. A particular problem with acquired resistance is that it can frequently affect drugs with unrelated mechanisms of action, with which the tumor may not yet have been treated. Resistance to chemotherapeutic drugs has been the subject of intense study and is known to occur at many levels, including changes in drug uptake or efflux, drug breakdown, alterations in the drug target, changes in the signaling pathways triggered by drug-induced damage, and attenuation of the apoptotic response (Longley and Johnston, 2005).

Much attention recently has been focused on the use of profiles of gene expression in tumor samples to search for

SIGNIFICANCE

There are many examples of individual genes promoting resistance or sensitivity to common cytotoxic agents in individual cell lines, but there has been little systematic analysis across a broad range of cancers defining common pathways of drug resistance and sensitivity. The functional genomic screen reported here implicates ceramide metabolism as a key regulator of sensitivity to diverse chemotherapeutic drugs. It also suggests a common mechanism promoting resistance to paclitaxel involving genes whose inhibition leads to induction of aneuploidy prior to drug treatment. This is consistent with the failure of taxanes to demonstrate clinical benefit in certain cancers with high rates of chromosomal instability and data demonstrating that low numerical chromosomal heterogeneity may predict responsiveness to these drugs in oncological practice.

correlations between expression of specific genes and acquisition of drug resistance in the clinic. This approach has been used to predict the outcome of therapy but may also provide indirect mechanistic insights into how drug resistance arises (Alaoui-Jamali et al., 2004; Lonning et al., 2005). However, obtaining sufficient numbers of high-quality tumor samples, whose drug sensitivity is known, in order to make strong correlations with expression of particular genes has proved challenging. It may be that far greater numbers of tumor samples need to be analyzed than previously assumed (Ein-Dor et al., 2006). One way around this has been to analyze gene expression in large numbers of cancer cell lines with known drug sensitivity (Potti et al., 2006). An alternative approach is taken here to assess more directly the contribution of over 800 candidate proteins to the sensitivity or resistance of cancer cells to a number of common chemotherapeutic drugs.

The ability to use RNA interference as a tool for gene silencing in mammalian cells has opened up the possibility of carrying out high-throughput loss-of-function screens in tissue culture systems (MacKeigan et al., 2005). Here we utilize a collection of synthetic siRNA oligonucleotide pools targeting the expression of all protein kinases, plus associated proteins and proteins involved in ceramide lipid metabolism, to address whether loss of these proteins impacts on drug sensitivity in vitro. The screen has been carried out in three commonly studied tumor cell lines with mutations in the *KRAS* oncogene and has employed four different chemotherapeutic drugs. We report that targeting *COL4A3BP* caused the most striking multidrug sensitization. This gene encodes a ceramide-binding protein, CERT, that is involved in transport of the proapoptotic lipid ceramide from its site of de novo synthesis in the endoplasmic reticulum to the Golgi, where it is metabolized to sphingomyelin (Hanada et al., 2003). We define a set of drug resistance genes that, when silenced, cause resistance to paclitaxel in multiple cell lines, many of which are involved in the spindle assembly checkpoint. These share the ability not only to impair paclitaxel-induced mitotic arrest, but also to induce polyploidy in the absence of drug exposure. These data suggest that taxanes may lack efficacy in tumors with high levels of chromosomal instability (CIN) characterized by chromosomal numerical heterogeneity and provide a rational basis for identification of patients likely to benefit from these drugs.

RESULTS

Kinases Affecting Cell Viability in the Absence of Drug Treatment

HCT-116 (HCT) colon carcinoma, MDA-MB-231 (MDA) breast adenocarcinoma, and A549 non-small-cell lung carcinoma cells were transfected with 779 synthetic siRNA pools targeting all human protein kinases, plus a number of kinase-associated and kinase-related proteins. Transfections were performed in duplicate for each of three conditions per cell line: vehicle-treated control (DMSO), paclitaxel-treated, and a custom drug treatment that was cell type specific (5-FU for HCT-116, doxorubicin for MDA-MB-231, and cisplatin for A549). Cells were transfected, followed 48 hr later with drug treatment for a further 48 hr, before cell viability was measured using the CellTiter-Glo assay. A concentration of drug was used that allowed identification of both siRNAs protecting cells and those giving enhanced killing in the same screen.

To assess viability effects induced by the siRNAs in the absence of drug, we analyzed data obtained from DMSO-treated transfections. 14 genes were identified whose knockdown significantly decreased cell number compared to scrambled control in at least two different cell lines (Figure 1A). Five siRNAs promoted an increase in viability in at least two different cell lines. A heatmap (Figure S1A in the Supplemental Data available with this article online) shows all siRNAs with a significant effect on cell viability detected in this screen. Those siRNAs with a statistically significant reduction in cell viability >25% averaged across all three cell lines are listed in graphical format in Figure S1B.

Four of the five top viability targets, *CNKSR1* (the adaptor protein CNK required for Ras signaling), *FN3KRP*, *EPHA6*, and *COPB2* (Figure S1B), were readily validated, with at least two of the four siRNAs in each pool promoting a significant reduction in viability in at least two cell lines (Figure S1C). The Vi-CELL trypan blue exclusion assay (Beckman Coulter) confirmed that gene silencing reduced cell viability by more than 20% (Figure S1D). Data from the gene expression database Oncomine (http://www.oncomine.org/) indicated that, of these genes, *COPB2* appeared to be significantly upregulated in various tumors compared to normal tissues (Figures S1E and S1F), raising the possibility that it could be a tumor-selective target.

Kinases Involved in Resistance to Paclitaxel Treatment

To identify proteins whose knockdown promoted a drug-sensitizing or -antagonistic phenotype, we analyzed data obtained after drug treatment, utilizing the sensitivity index (SI) equation. Figure 1B shows all siRNAs that alter drug action in at least one of the three cell lines. siRNAs against *BUB1B* and *CDADC1* can be readily identified as antagonizing the paclitaxel response in all cell lines tested.

Forty-three siRNAs with statistically significant paclitaxel antagonistic activity in two or more cell lines were identified (Table S1). These genes were categorized (Figure 2A) using gene ontology databases, available literature, and published RNAi screens in *Drosophila* (FLIGHT database, http://www.flight.licr.org/) and *C. elegans* (Bettencourt-Dias et al., 2004; Moffat et al., 2006; Whitfield et al., 2002). Genes with mitotic related function formed the most frequent group. Homologs of ten of these genes displayed mitotic phenotypes when knocked down in *Drosophila*, while overall 18/43 (42%) of these targeted genes have been associated with functions at the G2/M transition (Bettencourt-Dias et al., 2004; Eggert et al., 2004; Moffat et al., 2006).


A
A M H
CNKSR1
COPB2
CSK
EPAC
EPHA6
ERN1
FN3KRP
MAP2K3
NEK9
NME3
NPR2
PDGFRB
PFKL
SSH3BP1
CSNK1G3
DKFZP761P0423
GAP43
GNE
ULK3
Rc/Cc
0.2-0.3
0.3-0.4
0.4-0.5
0.5-0.6
Rc/Cc
1.5-1.6
1.4-1.5
1.3-1.4
1.2-1.3
B
Paclitaxel
Custom
A M H C D F
Sensitization (SI)
0.10-0.15
0.15-0.20
0.20-0.30
>0.3
Antagonism (SI)
-0.15 - -0.2
-0.20 - -0.3
-0.30 - -0.4
<-0.4

To validate these targets, we reassayed 16 siRNAs found to antagonize paclitaxel in two or more cell lines, eight siRNAs with an antagonistic phenotype in HCT-116 cells alone (Table S2), and two in MDA-MB-231 cells alone. The degree of antagonism to paclitaxel is portrayed in color-coded or graphical format from 10% to 50% (Figures S2A–S2D). We validated 25 of 26 of these selected antagonistic siRNAs in at least one cell line, with ten validated in all three cell lines and another eight in two different cell lines (Figure 2B). All validated paclitaxel antagonists promoted an increase in relative cell number following paclitaxel treatment (Figures S2B–S2D). Knockdown of each gene was confirmed by RT-PCR (Figure S2E).

Effects on Mitotic Index

Antagonism of paclitaxel activity is likely to result in reduced mitotic arrest in the presence of drug. We examined the cell-cycle profile following transfection of each of the validated paclitaxel-antagonistic siRNAs and quantified the mitotic index following paclitaxel treatment, defined as the percentage of MPM-2-phosphoepitope-positive cells. In control-transfected HCT-116 cells, over 60% of the entire population were MPM-2 positive following 18 hr of paclitaxel treatment. This compared to just 3.5% MPM-2-positive cells following DMSO treatment (Figure 2C). In contrast, *BUB1B* siRNA reduced the percentage of MPM-2-positive cells to <5% after 18 hr of paclitaxel treatment, with potent effects also seen for the other spindle assembly checkpoint regulators, *AURKB* and *TTK*. All of the remaining paclitaxel antagonists also promoted a reproducible reduction in the mitotic index. Comparable effects were also seen in both A549 and MDA-MB-231 cells (Figure S2F).

We investigated whether expression of the MDA-MB-231 paclitaxel antagonists were reduced in taxane-resistant primary breast cancer. A microarray study of patients with primary breast cancer treated with neoadjuvant docetaxel showed significantly lower expression levels of STK25 and DGUOK in patients with resistant disease ($p = 0.02$ and 0.00027, respectively) (Chang et al., 2003). *STK25* siRNA promoted paclitaxel resistance in both A549 and MDA-MB-231 cells (Figures S2B and S2C) and attenuated the induction of apoptosis and significantly increased BrdU incorporation in paclitaxel-treated cells in comparison to control cells (data not shown).

Polyploidy Induction and Multinucleation

We reasoned that, since all the paclitaxel antagonists reduced the mitotic index in the presence of drug, they might cause spindle checkpoint defects and induce polyploidy in the absence of paclitaxel. Accumulating evidence implies that the mitotic delay in response to spindle disruption influences the postmitotic p53-dependent G1 checkpoint, thereby arresting cells with tetraploid DNA (Blagosklonny, 2006; Vogel et al., 2004). HCT-116 cells provided an ideal model to study this relationship owing to their near-diploid status and retention of wild-type p53.

The siRNAs with the most potent effect on the mitotic arrest in HCT-116 cells following paclitaxel treatment (>75% reduction; Figure 2C) also induced polyploidy without drug by at least 4-fold (*BUB1B*, *CDC2*, *TTK*, *AURKB*, *EEF2K*, and *MASTL*; Figure 2D). In total, 17/20 of the siRNAs with paclitaxel antagonistic activity in HCT-116 cells displayed a reproducible increase in polyploidy (>1.5-fold) without drug treatment (Figure 2D and Figure 3). The reciprocal relationship between the potency of the mitotic arrest induced by paclitaxel and polyploidy without drug supports the interplay between the mitotic and G1 checkpoints (Vogel et al., 2004). The induction of polyploidy by antagonistic siRNAs was less pronounced in the A549 and MDA-MB-231 cells without drug; however, eight of these siRNAs appear to be permissive for polyploidy development following paclitaxel treatment (Figure S2G and Figure 3). This provides evidence that cells were passing through mitosis during paclitaxel treatment, indicating that paclitaxel antagonism was not due to inhibition of mitosis entry. In keeping with the involvement of polyploidy development in the acquisition of paclitaxel resistance, HCT-116 polyploid cells were still capable of synthesizing DNA as assessed by BrdU incorporation with paclitaxel (Figure S2H).

The observed induction of polyploidy prompted an analysis of centrosome and nuclear abnormalities following transfection of the individual paclitaxel antagonists into HCT-116 cells (Figure 3 and Figure S2I). Multinucleation was seen with many of the antagonistic siRNAs in the absence of drug, including *AURKB*, *BUB1B*, *CDC2*, *CSNK1A1*, *CSNK1A1L*, *EEF2K*, *MASTL*, and *TTK*. An increase in the number of cells with giant nuclei (>2-fold increase in nuclear diameter) was observed with all of the siRNAs inducing a multinuclear phenotype. In all cases where changes in nuclear phenotype were observed, parallel changes in centrosome size (>2-fold increase in centrosomal size) or number (>3 centrosomes/nucleus) were also apparent.

We addressed whether the most potent inducers of polyploidy could alter levels of mitotic regulators in the

Figure 1. Human Kinome Library Screen Primary Analysis

The screen set-up, data analysis, and hit selection are described in the Experimental Procedures.

(A) Shown are kinases, silencing of which affected viability compared to negative control in at least two cell lines (A549 [A], MDA-MB-231 [M], and HCT-116 [H]). Rc/Cc values are represented using a color-coding format (greens for decreased, reds for increased viability; white for no statistically significant changes).

(B) Figure represents kinases, knockdown of which altered drug activity (sensitivity index [SI]). Columns 1 to 3: SI to paclitaxel in A549, MDA-MB-231, and HCT-116 cells. Columns 4 to 6: SI to cisplatin (C) in A549, doxorubicin (D) in MDA-MB-231, 5-FU (F) in HCT-116 cells. SI are shown using a color-coding format (greens for sensitizing, reds for antagonizing siRNAs; white for no statistically significant changes).

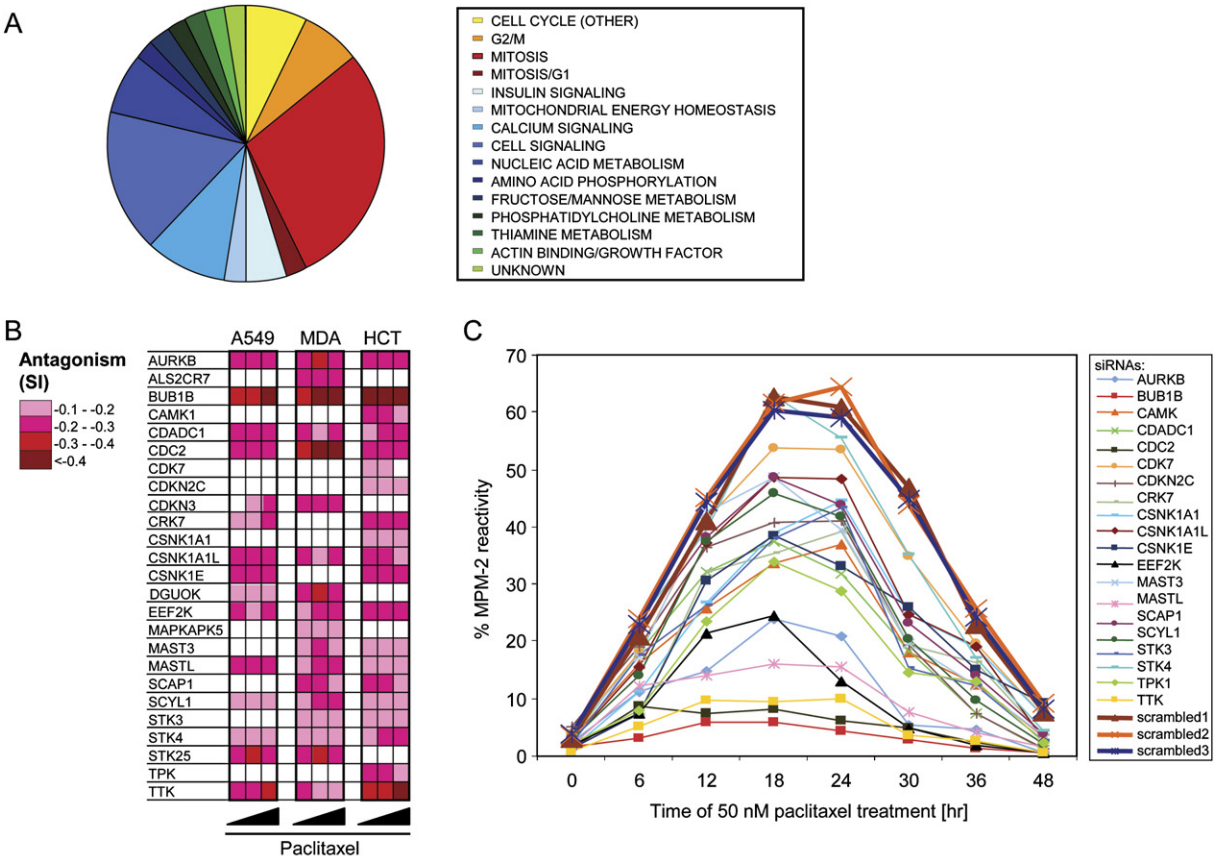
A
CELL CYCLE (OTHER)
G2/M
MITOSIS
MITOSIS/G1
INSULIN SIGNALING
MITOCHONDRIAL ENERGY HOMEOSTASIS
CALCIUM SIGNALING
CELL SIGNALING
NUCLEIC ACID METABOLISM
AMINO ACID PHOSPHORYLATION
FRUCTOSE/MANNOSE METABOLISM
PHOSPHATIDYLCHOLINE METABOLISM
THIAMINE METABOLISM
ACTIN BINDING/GROWTH FACTOR
UNKNOWN
B
Antagonism (SI)
-0.1 - -0.2
-0.2 - -0.3
-0.3 - -0.4
<-0.4
A549
MDA
HCT
AURKB
ALS2CR7
BUB1B
CAMK1
CDADC1
CDC2
CDK7
CDKN2C
CDKN3
CRK7
CSNK1A1
CSNK1A1L
CSNK1E
DGUOK
EEF2K
MAPKAPK5
MAST3
MASTL
SCAP1
SCYL1
STK3
STK4
STK25
TPK
TTK
Paclitaxel
C
% MPM-2 reactivity
Time of 50 nM paclitaxel treatment [hr]
siRNAs:
AURKB
BUB1B
CAMK
CDADC1
CDC2
CDK7
CDKN2C
CRK7
CSNK1A1
CSNK1A1L
CSNK1E
EEF2K
MAST3
MASTL
SCAP1
SCYL1
STK3
STK4
TPK1
TTK
scrambled1
scrambled2
scrambled3
D
DMSO
Paclitaxel
DNA content >4N (fold of control)
scrambled
CDADC1
CDK7
STK4
SCAP1
CAMK1
MAST3
CSNK1A1
CRK7
CSNK1E
SCYL1
CSNK1A1L
STK3
TPK1
CDKN2C
BUB1B
CDC2
TTK
AURKB
EEF2K
MASTL
E
Bub1B expression
Relative image density (fold of control)
Time of paclitaxel [hr]
scrambled
EEF2K
MASTL
BUB1B
TTK
F
Cyclin B1 expression
G
Paclitaxel [hr]
PThr308-Akt
PSer473-Akt
loading
H
siRNA
Paclitaxel
sc
MASTL
BUB1B
TTK
EEF2K
PSer473-Akt
loading

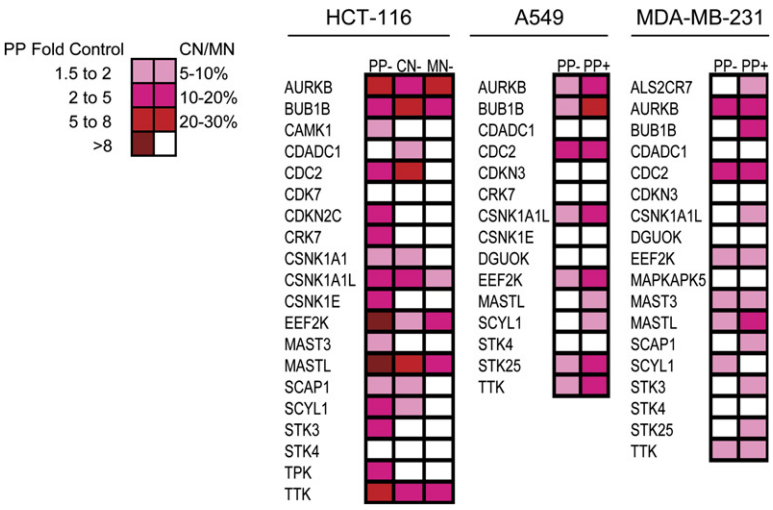

Figure 3. Induction of Polyploidy and Karyotypic Abnormalities by Paclitaxel-Antagonistic siRNAs

Cells were transfected with paclitaxel antagonistic siRNAs. Strength of polyploidy induction is represented in color-coded format with (PP+) and without (PP−) paclitaxel treatment. Microscopy data are quantified for HCT-116 cells, showing percentage of cells with centrosome abnormalities in size or number (CN) and those displaying multinucleation (MN) in the absence of drug.

presence of paclitaxel. We examined the expression of cyclin B1, whose degradation is tightly regulated by the status of the spindle checkpoint and BUB1B, a key component of the mitotic spindle machinery after transfection of HCT-116 cells with selected siRNAs, which demonstrated the most potent effect on polyploidy induction and mitotic index reduction with paclitaxel. Following paclitaxel treatment of control-transfected cells, we observed an increase in both BUB1B and cyclin B1 protein that reached a maximum after 18–24 hr (Figures 2E and 2F), coincident with maximal MPM-2 reactivity observed by flow cytometry. This increase in cyclin B1 and BUB1B protein expression was markedly attenuated by *BUB1B*, *EEF2K*, *MASTL*, and *TTK* knockdown (Figure 2C). Premature cyclin B1 degradation may reflect spindle checkpoint inactivation and mitotic slippage. Reduced BUB1B expression may result in impaired APC/C inhibitory activity weakening the spindle checkpoint response.

Activation of Akt/PKB has been suggested to play a role in the induction of aneuploidy and multinucleation of HEK293 cells (Jin and Woodgett, 2005). We found that the phosphorylation of Akt Ser473 and Thr308 was reduced following paclitaxel treatment in control-transfected cells (Figure 2G). In contrast, in *MASTL*, *BUB1B*, *TTK*, and *EEF2K* siRNA-transfected cells, treatment with paclitaxel for 18 hr did not induce a significant reduction of phosphorylated Akt (Figure 2H). Sustained Akt activity may attenuate drug-induced apoptosis, thereby promoting paclitaxel resistance; however, elevated Akt activity in the presence of paclitaxel could be a downstream consequence of failure of mitotic arrest rather than a cause of it.

We asked whether chromosomal numerical heterogeneity (NH), a putative karyotypic marker of a defective mitotic checkpoint, could be used as a phenotypic marker for intrinsic paclitaxel resistance in the colorectal cancer (CRC) or breast cancer (BC) cell lines of the NCI-60 cancer cell line panel. We used publicly available karyotypic abnormality data for the NCI-60 CRC and BC cell lines (Roschke et al., 2003) and growth inhibitory data (GI50) derived from the Developmental Therapeutics Program data repository (http://dtp.nci.nih.gov/; http://www.broad.mit.edu/mpr/NCI60) to determine the correlation between NH and drug response. Figure S2J demonstrates that microtubule-stabilizing agents (paclitaxel and halichondrin B) or mitotic Eg5 inhibitors (NSC56817 and Trityl-cysteine) may be less efficacious in CRC or BC cell lines with high chromosomal numerical heterogeneity (GI50:NH correlation coefficients 0.64–0.87). Drugs with established activity in CRC (with high-frequency CIN), such as oxaliplatin and irinotecan (CPT-11), displayed negative correlation coefficients (−0.54 and −0.71), indicating that these non-microtubule-targeting agents may have superior efficacy in cell lines with high NH.

Figure 2. Identification of Kinases Involved in Resistance to Paclitaxel Treatment

(A) Forty-three siRNAs inducing an antagonistic response to paclitaxel in at least two cell lines were classified according to gene function using Gene Ontology groups and available literature and by comparing gene homologs in *D. melanogaster* using the Flight database. (B) Represented are 25 kinases, knockdown of which had a validated antagonistic effect on paclitaxel action. SI are shown using a color codes for three different concentrations of paclitaxel in the three cell lines. (C) Forty-eight hours after siRNA transfection, HCT-116 cells were treated with DMSO or 50 nM paclitaxel. Cells were analyzed for MPM-2 reactivity by flow cytometry. Data are expressed as percent of MPM-2-reactive cells in the propidium iodide (PI)-positive population. A representative experiment is shown. (D) Transfected HCT-116 cells were treated with DMSO or 50 nM paclitaxel for 48 hr. Cells were analyzed for >4N DNA content by flow cytometry. Data are expressed as fold of DMSO-treated scrambled control of the percent of cells with DNA content >4N in the PI positive population, each value representing the average (+SEM) from three independent experiments. (E, F, and H) Transfected HCT-116 cells were treated with paclitaxel for the indicated times (E and F) or 18 hr (H), and western blot analysis was performed to detect BUB1B (E), Cyclin B1 (F), and phospho-Akt (H) expression. Bands were analyzed by scanning densitometry, the signal was normalized to the GAPDH levels, and the ratio to scrambled control-treated samples was calculated (E and F). (G) HCT-116 cells were treated for the indicated times with 50 nM paclitaxel, and western blot was performed to detect phospho^{Ser473}- and phospho^{Thr308}-Akt.

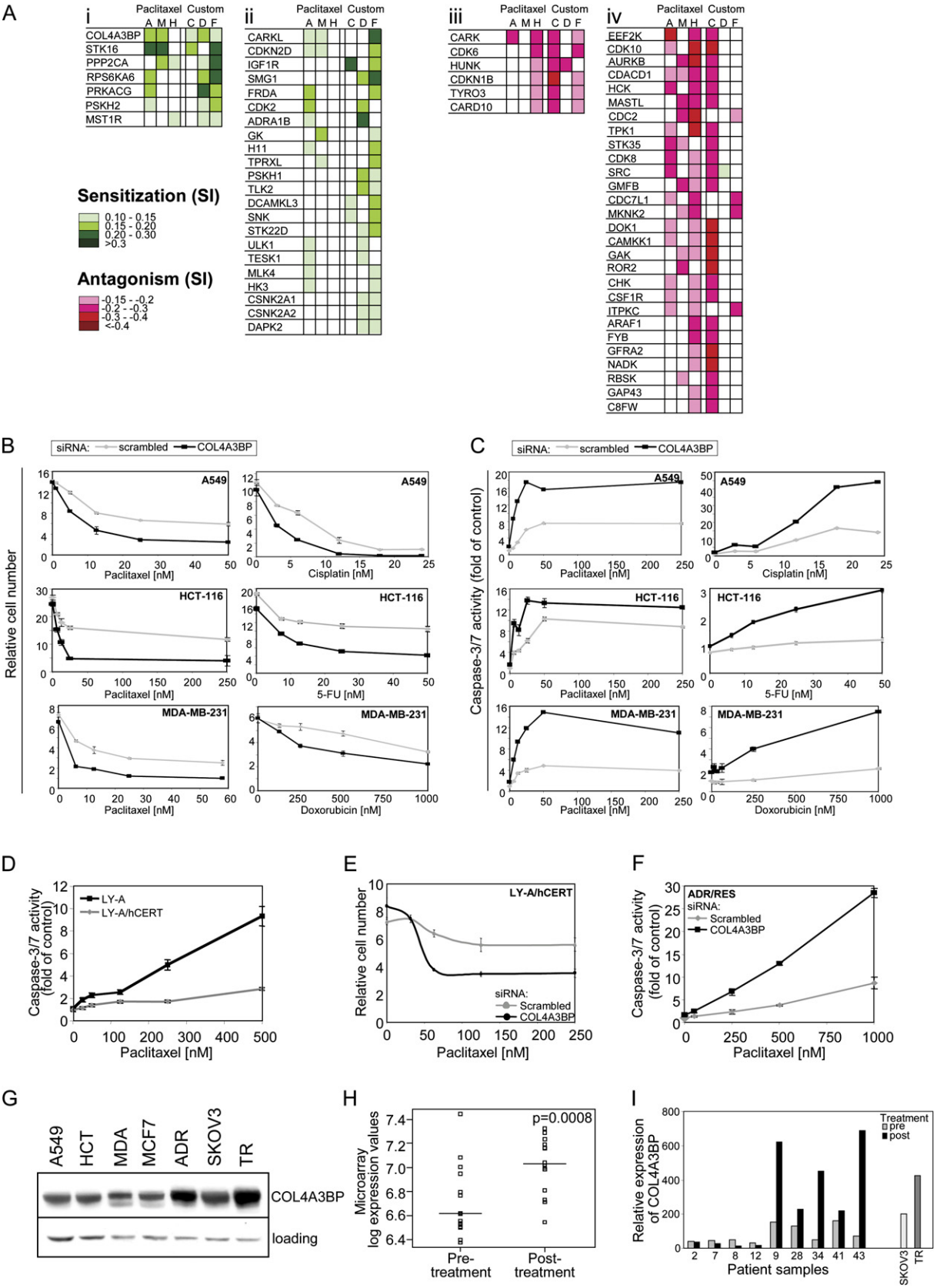
A
i
Paclitaxel Custom
A M H C D F
COL4A3BP
STK16
PPP2CA
RPS6KA6
PRKACG
PSKH2
MST1R
ii
CARKL
CDKN2D
IGF1R
SMG1
FRDA
CDK2
ADRA1B
GK
H11
TPRXL
PSKH1
TLK2
DCAMKL3
SNK
STK22D
ULK1
TESK1
MLK4
HK3
CSNK2A1
CSNK2A2
DAPK2
iii
CARK
CDK6
HUNK
CDKN1B
TYRO3
CARD10
iv
EEF2K
CDK10
AURKB
CDACD1
HCK
MASTL
CDC2
TPK1
STK35
CDK8
SRC
GMFB
CDC7L1
MKNK2
DOK1
CAMKK1
GAK
ROR2
CHK
CSF1R
ITPKC
ARAF1
FYB
GFRA2
NADK
RBSK
GAP43
C8FW
Sensitization (SI)
0.10 - 0.15
0.15 - 0.20
0.20 - 0.30
>0.3
Antagonism (SI)
-0.15 - -0.2
-0.2 - -0.3
-0.3 - -0.4
<-0.4
B
siRNA: scrambled COL4A3BP
Relative cell number
A549
Paclitaxel [nM]
Cisplatin [nM]
HCT-116
5-FU [nM]
MDA-MB-231
Doxorubicin [nM]
C
siRNA: scrambled COL4A3BP
Caspase-3/7 activity (fold of control)
D
LY-A
LY-A/hCERT
Caspase-3/7 activity (fold of control)
Paclitaxel [nM]
E
LY-A/hCERT
siRNA:
Scrambled
COL4A3BP
Relative cell number
F
ADR/RES
siRNA:
Scrambled
COL4A3BP
G
A549
HCT
MDA
MCF7
ADR
SKOV3
TR
COL4A3BP
loading
H
Microarray log expression values
p=0.0008
Pre-treatment
Post-treatment
I
Relative expression of COL4A3BP
Treatment
pre
post
Patient samples
SKOV3
TR

In the management of metastatic breast cancer, the combination of trastuzumab (Herceptin) and paclitaxel increases the clinical benefit compared to paclitaxel alone (Slamon et al., 2001). We asked whether this clinical benefit might be attributable to downregulation of genes implicated in CIN following HER2 blockade. We compared the 70 gene microarray signature data set associated with CIN (Carter et al., 2006) with an in vitro data set of 16 genes repressed by anti-HER2 antibody (Le et al., 2005) and found 8 of these 16 genes to be represented in the CIN signature set ($p = 2.3 \times 10^{-16}$: probability of observing 8 or more genes in the top 70 [of 10,151 genes] when tested using the hypergeometric test based on the 16 [out of 12,558] differential genes on the U95A version 2 chip).

In summary, while all of the validated paclitaxel-antagonistic siRNAs reduced the proportion of cells arrested in mitosis in response to paclitaxel treatment, most of them also induced polyploidy, multinucleation, and abnormalities of centrosome size or number in the absence of drug. This suggests a possible mitotic regulatory role for these genes and an association between CIN and paclitaxel resistance. Supporting a role for polyploidy in the acquisition of paclitaxel resistance, polyploid cells continued to synthesize DNA in the presence of paclitaxel, and increasing chromosomal numerical heterogeneity correlated with increasing resistance to paclitaxel in breast and colon cancer cell lines.

Identification of a Multidrug-Sensitizing siRNA Targeting *COL4A3BP*

Resistance of tumors to unrelated cytotoxics results in early treatment failure, limiting therapeutic options in the clinical setting. To define genes potentially influencing sensitivity to diverse cytotoxics, we calculated the average SI across the three cell lines with all four drugs for each siRNA. Figure 4Ai and Figure S3A demonstrate that siRNAs targeting *COL4A3BP* and *STK16* sensitized cells to most conditions used in this screen.

We validated *COL4A3BP* siRNA as a multidrug sensitizer reproducing the results from the primary screen (Figures 4B and 6B; data not shown). *COL4A3BP* siRNA promoted a synergistic increase in caspase-3/7 activity in the presence of paclitaxel in all three cell lines and to doxorubicin in MDA-MB-231, 5-FU in HCT-116, and cisplatin in A549 cells (Figure 4C). Efficient knockdown of protein expression was seen in each cell line and with each of the deconvoluted siRNAs (Figures S3B and S3C).

COL4A3BP (also known as CERT) transports ceramide in a nonvesicular manner from the ER to the Golgi apparatus and was identified as a factor defective in LY-A cells, a CHO cell derivative deficient in sphingomyelin due to a mutation impairing COL4A3BP's Golgi targeting function (Hanada et al., 2003). We found that LY-A cells appeared to be more sensitive to paclitaxel compared to derivatives overexpressing human COL4A3BP (Figure 4D). Furthermore, knocking down *COL4A3BP* with siRNA sensitized LY-A/hCERT cells to paclitaxel (Figure 4E).

The drug resistance properties of ADR/RES cells are thought to be partially attributable to overexpression of glucosylceramide synthase (GCS) which converts ceramide to glucosylceramide (Gouaze et al., 2005), thereby affecting overall ceramide levels in the cell. To determine whether disruption of ceramide transport may play a role, we challenged ADR/RES cells with paclitaxel following transfection of *COL4A3BP* siRNA. Paclitaxel sensitization was observed in parallel with a rise in caspase-3/7 activity compared to control cells (Figure 4F). Western analysis demonstrated that COL4A3BP protein expression was increased in ADR/RES cells compared to the cells used in the screen and MCF-7 cells (originally thought to be the parent line for ADR/RES). The paclitaxel-resistant ovarian cancer cell line SKOV3-TR also expressed higher levels of COL4A3BP compared to the parent cell line, SKOV3 (Figures 4G and 4I).

COL4A3BP Expression Is Increased in Ovarian Cancer Samples after Paclitaxel Treatment

We identified *COL4A3BP* as a candidate paclitaxel resistance gene in samples from the CTCR-OV01 prospective randomized study of chemotherapy response in ovarian cancer using supervised analysis of Affymetrix U133A expression data (A.A.A. and J.D.B., unpublished data). Data from 14 evaluable paired samples from patients receiving three cycles of neoadjuvant paclitaxel showed increased *COL4A3BP* expression after drug treatment ($p = 0.0008$, paired Student's t test; Figure 4H). qRT-PCR for *COL4A3BP* from available RNA from nine of these pairs is demonstrated in Figure 4I. This showed that the mean

Figure 4. Identification of Kinases Involved in Multidrug Sensitization and Resistance

(A) Screen data for kinases that affected sensitivity to more than one drug following knockdown. Shown are siRNAs sensitizing to three or more (Ai) or two cytotoxics (Aii) or antagonistic to three or more (Aiii) or two cytotoxics (Aiv). SI (color coded: greens, sensitizing siRNAs; reds, antagonizing siRNAs; white, no statistically significant changes) are shown to paclitaxel (columns 1 to 3) and to custom drug (columns 4 to 6).

(B and C) Cells were treated 48 hr after transfection with *COL4A3BP* or scrambled siRNA for 48 hr. Relative cell numbers were measured using CellTiter-Glo assay (B). Caspase-3/7 activity was quantified by APO-1 assay and normalized for cell number and is expressed as fold of untreated negative control siRNA-transfected sample (C). Shown are results of representative experiments with mean ± SD.

(D) LY-A and LY-A/hCERT cells were treated for 48 hr with paclitaxel. Caspase-3/7 activity was assessed as in (C).

(E and F) LY-A/hCERT (E) and ADR/RES (F) cells were transfected, treated, and analyzed as described in (B) and (C).

(G) Western blot analysis of cell lysates of indicated cells (with ADR = ADR/RES and TR = SKOV3/TR cells) detecting COL4A3BP and GAPDH expression.

(H and I) OV01 microarray analysis: in a prospective randomized study of chemotherapy response in ovarian cancer, 14 paired samples from patients receiving three cycles of neoadjuvant paclitaxel were used to perform a microarray using Affymetrix U133A. Expression data were analyzed for COL4A3BP expression before and after paclitaxel treatment (H). RNA from nine paired samples and SKOV3 and SKOV3-TR cells was analyzed for COL4A3BP expression by qPCR (I).

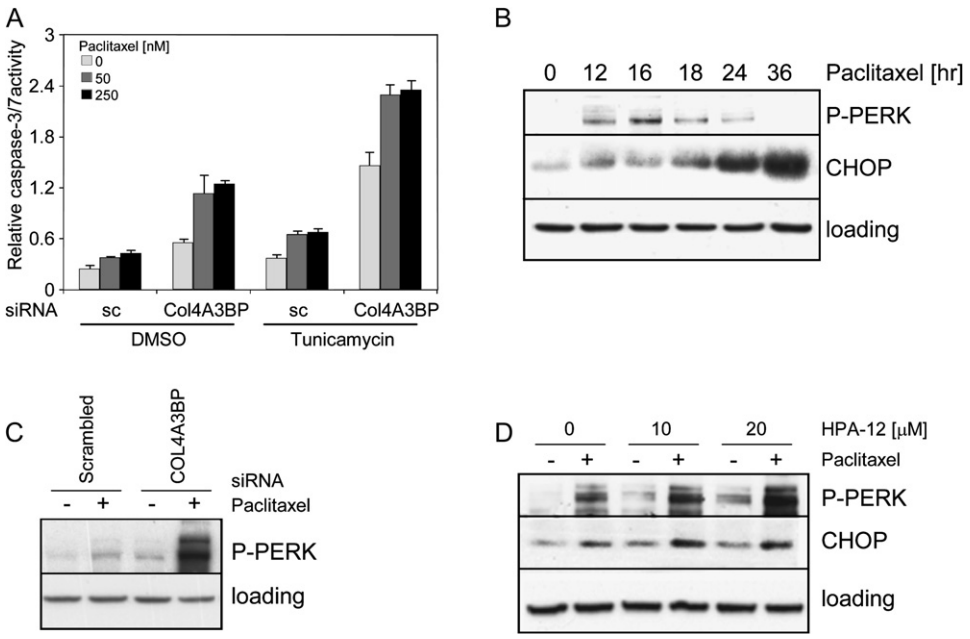

Figure 5. ER Stress Response

(A) Forty-eight hours after transfection with *COL4A3BP* or scrambled siRNAs, HCT-116 cells were treated with 1 μg/ml tunicamycin for 18 hr. Caspase-3/7 activity was quantified using the APO-1 assay and normalized for cell number. Data are shown as mean + SD.

(B) HCT-116 cells were treated with 50 nM paclitaxel, and western blot analysis was performed to detect phospho-PERK and CHOP.

(C) Forty-eight hours after transfection of HCT-116 cells with *COL4A3BP* or scrambled siRNAs, cells were treated with 50 nM paclitaxel for 24 hr, and western blot analysis was performed to detect phospho-PERK.

(D) HCT-116 cells were treated for 15 min with HPA-12 or DMSO at 4°C, followed by 2 hr paclitaxel treatment. Phospho-PERK and CHOP were detected by western blotting.

expression increased >3-fold in posttreatment versus pretreatment tumors (p = 0.07, paired Student's t test). Taken together, these studies provide early clinical correlates for COL4A3BP overexpression and drug resistance.

COL4A3BP Knockdown Augments ER Stress

Many chemotherapeutic agents, including paclitaxel, induce CHOP/GADD153 expression, an apoptotic regulator of the ER stress response. Increased CHOP mRNA correlates with response to paclitaxel in primary breast cancer (de las Alas et al., 2000). Conceivably, impaired ceramide transport as a result of COL4A3BP inhibition might promote an increase of ceramide in the ER, thereby promoting ER stress, which might in turn sensitize cells to paclitaxel treatment.

Supporting this hypothesis, we found that knockdown of *COL4A3BP* promoted a synergistic increase in caspase activity (Figure 5A) in the presence of tunicamycin (an ER stress-inducing agent) and an increase in sub-G1 DNA content in comparison to cells treated with tunicamycin or *COL4A3BP* siRNA alone (data not shown). Treatment of HCT-116 cells with paclitaxel induced PERK phosphorylation within 4 hr (data not shown) reaching maximal levels at 16 hr (Figure 5B). CHOP expression was also induced between 18 and 24 hr after paclitaxel treatment. A similar induction of both PERK phosphorylation and CHOP expression was also noted in MDA-MB-231 and A549 cells in response to paclitaxel (data not shown).

Given the ability of *COL4A3BP* knockdown to sensitize cells to ER stress induced by tunicamycin, we asked whether *COL4A3BP* silencing or pharmacological inhibition of COL4A3BP by HPA-12 could potentiate ER stress both alone and with paclitaxel. Knockdown of *COL4A3BP* alone in HCT-116 cells induced an increase in PERK phosphorylation comparable to the paclitaxel-induced increase (Figure 5C). Treatment with paclitaxel following *COL4A3BP* silencing further significantly increased PERK phosphorylation (Figure 5C). PERK phosphorylation was also increased in HCT-116 cells treated with HPA-12 (Figure 5D), supporting the dependence of ER stress on ceramide transport activity in these cells.

These data confirm the ability of paclitaxel to induce markers of ER stress and suggest a mechanism whereby *COL4A3BP* knockdown augments both basal markers of ER stress and ER stress induction in response to paclitaxel treatment.

Systematic Analysis of Ceramide Regulators

Given the role of COL4A3BP in ceramide transport and its multidrug-sensitizing properties, we attempted to define whether knockdown of other enzymes influencing the metabolism of ceramide altered drug sensitivity. We challenged HCT-116, MDA-MB-231, and A549 cells treated with paclitaxel, doxorubicin, 5-FU, or cisplatin with a "ceramidome" siRNA library targeted to the known enzymatic regulators of the pathway including those involved in the

de novo synthesis of ceramide and sphingomyelin hydrolysis. siRNAs inducing a statistically significant phenotype are shown in Figure S4A. Figure 6A depicts each of the enzymes involved in ceramide and sphingomyelin metabolism with the gene name(s) adjacent in color-coded format, indicating sensitization or antagonism by their targeting siRNA in two or more cell lines. *COL4A3BP* siRNA sensitized the three cell lines to 9 out of 12 conditions. No other siRNA-targeting molecules involved in ceramide metabolism had such a profound effect on drug sensitivity.

We chose to further investigate *GBA* (β-glucosidase), as this was the only siRNA that promoted resistance to paclitaxel in all three cell lines. GBA converts glucosylceramide into ceramide, opposing the action of glucosylceramide synthase. The *GBA* siRNA promoted paclitaxel antagonism in all three cell lines (Figure 6B). Efficient knockdown of GBA protein was observed (Figure S4B).

Next we addressed whether pharmacological inhibition or manipulation of the ceramide pathway using selected siRNAs could influence a mitotic arrest induced by paclitaxel. Pretreatment of HCT-116 cells with C_6-ceramide increased paclitaxel-induced mitotic arrest (Figure 6C). Inhibition of COL4A3BP by HPA-12 (Kumagai et al., 2005) or silencing by siRNA accentuated a mitotic arrest as early as 2 hr following paclitaxel treatment (Figures 6C and 6D).

In common with the other paclitaxel antagonists found in this screen, *GBA* siRNA reduced the induction of MPM-2 reactivity after paclitaxel treatment in the three cell lines (Figure 6D). Furthermore, knockdown of another β-glucosidase, *GBA3*, also attenuated a mitotic arrest and promoted resistance to paclitaxel in HCT-116 cells (Figure 6E). These data suggest that alterations in nonvesicular ceramide transport or ceramide synthesis from glucosylceramide may affect the mitotic arrest induced by paclitaxel.

In keeping with many of the paclitaxel antagonists identified in this screen, *GBA* siRNA promoted an increase in polyploidy in all three cell lines without paclitaxel (Figure 6F). Furthermore, we noted significant induction of GBA protein at 12 hr following paclitaxel treatment (Figure 6G), suggesting that GBA induction may play a role in ceramide elevation involved in paclitaxel toxicity.

PI3K/Akt Inhibition Attenuates Development of Aneuploidy

As observed previously, following 24 hr treatment of HCT-116 cells with paclitaxel, levels of phosphorylated Akt were reduced in comparison to untreated control cells (Figures 2G and 7A). Knockdown of *COL4A3BP* further enhanced the loss of phosphorylated Akt, while knockdown of *GBA* prevented the paclitaxel-induced decrease of phosphorylated Akt levels.

The associations between PI3K pathway activation, CIN and taxane resistance, and the sustained activation of Akt in the presence of paclitaxel following transfection of polyploidy inducing paclitaxel antagonists prompted us to investigate whether inhibition of PI3K/Akt signaling could prevent the induction of aneuploid cells. Following transfection of *BUB1B* and *GBA* siRNAs, pretreatment with inhibitors of PI3K (LY294002) or Akt (inhibitors V and VIII) inhibited paclitaxel-induced aneuploidy development (Figure 7B). Analysis by flow cytometry showed that aneuploidy reduction is associated with an increased proportion of cells in the G1 and G2/M fraction of the cell cycle, which might indicate a 2N and 4N G1 arrest (data not shown). Therefore, it is possible that inactivation of Akt may induce a G1 cell-cycle arrest following mitotic slippage, thereby preventing endoreduplication of DNA and propagation of aneuploid progeny.

Topology of Akt Inactivation after *COL4A3BP* Inhibition

The mechanism whereby COL4A3BP inhibition, which induces ceramide accumulation in the ER (Hanada et al., 2003), might promote Akt inactivation by paclitaxel (Figure 7A) was explored. Activation of Akt is initiated by the binding of 3′ phosphorylated phosphoinositide lipids to its pleckstrin homology (PH) domain, promoting plasma membrane localization. We used HCT-116 cells expressing a construct in which GFP is fused to the Akt amino-terminal regulatory region that spans the PH domain (termed GFP-AH). As shown before, in untreated cells growing in serum this protein is localized to the plasma membrane (Watton and Downward, 1999). Figure 7C demonstrates that pretreatment of cells growing in serum with the COL4A3BP inhibitor HPA-12 significantly reduced the percentage of cells with membrane GFP-AH staining at 18 hr of paclitaxel treatment. The translocation of the Akt PH domain to the plasma membrane is thus influenced by ceramide accumulation in the ER.

DISCUSSION

Development of Aneuploidy and Resistance to Paclitaxel

A characteristic of all siRNAs promoting paclitaxel resistance in this study is a reduction in the accumulation of drug-treated cells at the mitotic checkpoint. This is expected, given the assumption that mitotic arrest induction is required for paclitaxel cytotoxicity: any mechanism reducing the efficacy of the drug is likely to be reflected in a reduction of the mitotic index in the presence of paclitaxel. Unexpectedly, however, most of these siRNAs also induced the appearance of polyploid cells, multinucleation, and centrosomal abnormalities without drug treatment. A significant number of mitotic regulators appeared as paclitaxel antagonists following knockdown, some of which have been implicated in sensitivity to microtubule-targeted drugs. The results of this screen support the concept that spindle checkpoint disruption promotes paclitaxel antagonism. The early mitotic spindle assembly checkpoint influences the postmitotic checkpoint following mitotic slippage, thereby preventing endoreduplication of DNA and the propagation of polyploid cells, which may contribute to aneuploidy (Blagosklonny, 2006; Shi and King, 2005; Vogel et al., 2004).

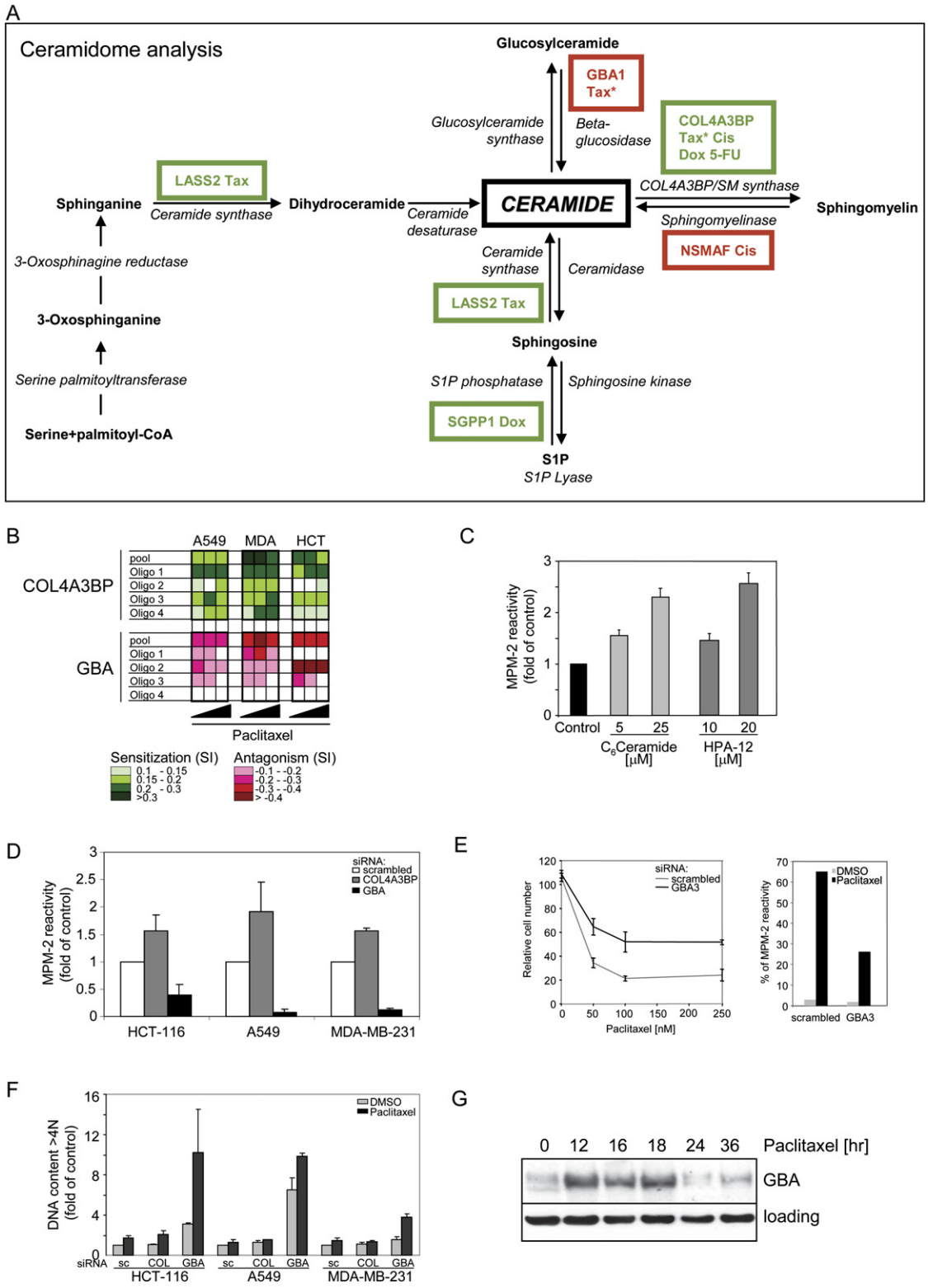

Figure 6. Ceramidome siRNA Screen

(A) A ceramidome siRNA screen was set up as the kinome screen. siRNAs inducing a phenotype in at least two cell lines are colored (sensitizing, green; antagonizing, red). Asterisk indicates phenotype observed in three cell lines.

(B) Cells were transfected with *COL4A3BP* or *GBA* siRNA pools or their four deconvoluted single siRNAs, treated with paclitaxel for 48 hr before CellTiter-Glo assay was performed. SI are shown using a color-coding format (antagonistic siRNAs, red; sensitizing siRNAs, green).

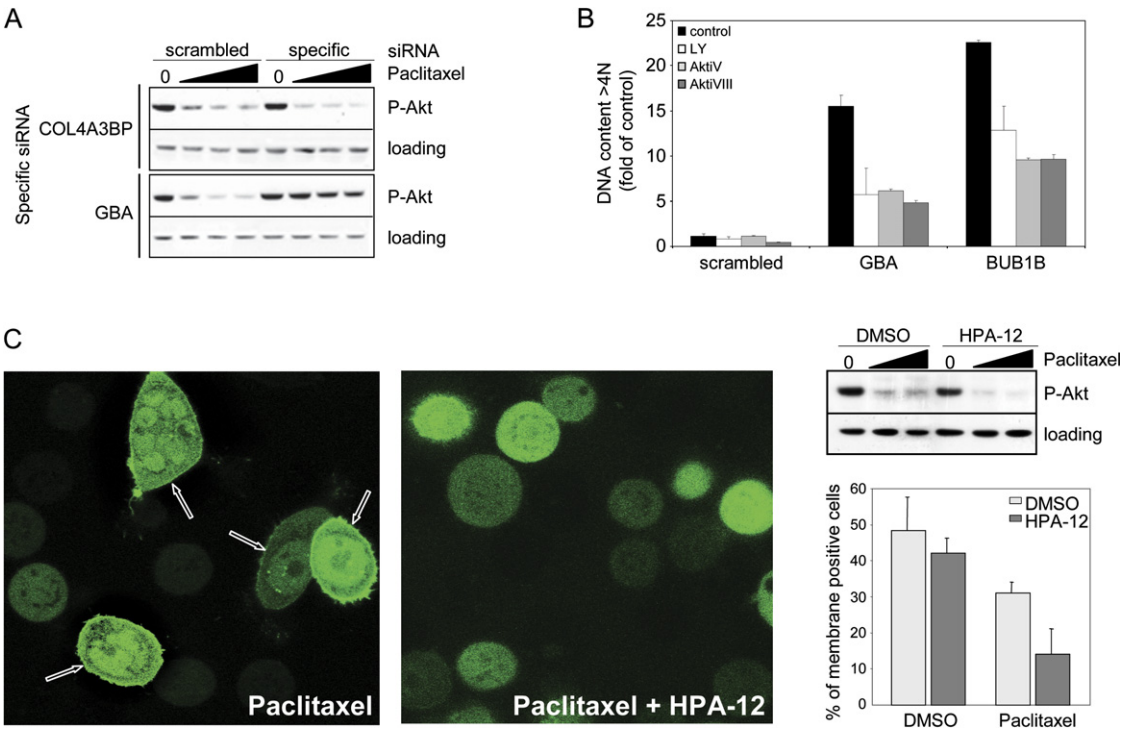

Figure 7. Akt Phosphorylation and Akt PH Domain Membrane Localization

(A) HCT-116 cells were transfected with *COL4A3BP*, *GBA*, or scrambled siRNA. Forty-eight hours later, cells were treated with paclitaxel for 18 hr, and phospho-Akt was detected by western blotting.

(B) Transfected HCT-116 cells were treated with DMSO, 10 μM LY294002 (LY), 0.3 μM Akt-inhibitor V (AktiV), or 1 μM Akt-inhibitor VIII (AktiVIII) for 1 hr followed by treatment with 50 nM paclitaxel for 18 hr. Cells were analyzed for >4N DNA content by flow cytometry. Data are expressed as mean fold change (+SEM) in the percentage of cells with >4N DNA in the PI-positive population relative to untreated scrambled control transfected cells.

(C) HCT-116 cells expressing GFP-AH were plated 8 hr prior to HPA-12 (20 μM) or DMSO treatment for 15 min at 4°C followed by treatment with 50 nM paclitaxel for up to 18 hr. Representative confocal microscopy images are shown on the left (arrows indicate membrane GFP-AH). On average 500 cells per condition were counted, and data shown (graph on the right) represent the mean percentage of cells (+SD) with membrane GFP-AH in four independent experiments. In parallel, HCT116 cells were treated with HPA-12 as above followed by treatment paclitaxel for 18 hr, and phospho-Akt or GAPDH expression was detected by western blotting.

This partly explains why disruption of selected spindle checkpoint regulators here not only reduces the mitotic index in the presence of microtubule stabilizers but also promotes the generation of polyploid cells, which continue to synthesize DNA in the 4N state.

The numerical chromosomal or centrosomal abnormalities in cancer cells that exist prior to treatment with microtubule-targeting drugs may serve as a phenotypic marker of intrinsic taxane resistance. Indeed, cells displaying CIN are more resistant to a mitotic arrest induced by microtubule inhibition than near-diploid cell lines with microsatellite instability (MSI+), and microtubule inhibitors are known to induce polyploidy and CIN in checkpoint-deficient or taxane-resistant cells (Cahill et al., 1998; Roberts et al., 1990; Shin et al., 2003; Vogel et al., 2004). Recently, it has been proposed that nondisjunction at mitosis triggers tetraploidy, which subsequently leads to aneuploid progeny due to a vastly increased rate of chromosome missegregation in tetraploid cells, potentially contributing to CIN (Shi and King, 2005). The correlation

(C) HCT-116 cells were treated for 1 hr with 5 or 25μM C_6Ceramide followed by 4 hr of 50 nM paclitaxel. In parallel, cells were treated for 15 min with HPA-12 at the indicated doses at 4°C before 2 hr of 50 nM paclitaxel. MPM-2 reactivity was assessed by flow cytometry. Data are expressed as mean fold change (+SEM) in the percentage of MPM-2-positive cells relative to paclitaxel-treated control cells.

(D) Cells were transfected with *COL4A3BP*, *GBA*, or scrambled siRNAs and 48 hr later treated with 50 nM paclitaxel for 18 hr. Data are expressed as mean fold change (+SEM) in the percentage of MPM-2-positive cells relative to paclitaxel-treated scrambled control transfected cells.

(E) HCT-116 cells were transfected with *GBA3* or scrambled siRNAs. Paclitaxel was added 48 hr posttransfection for 48 hr. Relative cell numbers were measured using CellTiter-Glo assay. In parallel HCT-116 cells were transfected as above and treated with 50 nM paclitaxel for 18 hr, and MPM-2 reactivity was analyzed by flow cytometry.

(F) Cells were transfected with *COL4A3BP*, *GBA*, or scrambled siRNAs. Forty-eight hours after transfection, cells were treated with DMSO or 50 nM paclitaxel for 18 hr. Cells were analyzed for >4N DNA content by flow cytometry. Data are expressed as mean fold change (+SEM) in the percentage of cells with >4N DNA relative to control cells.

(G) HCT-116 cells were treated with 50 nM paclitaxel for the indicated times. GBA expression was detected by western blotting.

between paclitaxel-induced polyploidy in K562 leukemia cells and paclitaxel resistance has prompted the suggestion that polyploidy in response to paclitaxel may be a useful indicator of drug resistance (Roberts et al., 1990). We extend this observation and suggest that genes that are permissive for polyploidy, when targeted by RNA interference, influence pathways that taxanes depend upon for cellular cytotoxicity, and that polyploidy or CIN prior to drug treatment may serve as a marker for de novo taxane resistance. Conversely, taxane treatment may select for a higher frequency of CIN in residual tumor.

These data suggest a compelling reason for the failure of taxanes to demonstrate activity in CRC, a disease with a high frequency of CIN. It also implies that 15% of CRCs, which are MSI+/near diploid, might be more sensitive to microtubule-stabilizing agents. Treatment of MSI+ patients with microtubule inhibitors is the focus of a clinical trial, CINATRA (chromosomal instability and anti-tubulin response assessment, Eudract number 2006-006073-24 and Supplemental Data).

Consistently, cells transfected with the siRNAs inducing the most potent induction of polyploidy without drug displayed elevated phosphorylated Akt following paclitaxel treatment. PI3K pathway deregulation has been shown to correlate with resistance to docetaxel (Potti et al., 2006). The highly significant ($p = 1.3 \times 10^{-21}$) representation of 16 genes in the PI3K predictor set in the CIN70 signature set suggests a role for PI3K activation and CIN (Potti et al., 2006; Carter et al., 2006). It is intriguing that 8 of the 16 genes significantly repressed by anti-HER2 antibody treatment are overexpressed in the CIN70 gene signature set ($p = 2.3 \times 10^{-16}$). The clinical studies demonstrating the impressive clinical benefit with taxanes and trastuzumab (Slamon et al., 2001) may be attributable to preferential repression by trastuzumab of genes promoting CIN.

Can spindle checkpoint disruption give long-term advantage to tumor cells in vivo in terms of taxane resistance? Prolonged major disruption of the spindle checkpoint is not tolerated by cells due to massive chromosome loss resulting in apoptosis (Kops et al., 2004). In a clinical setting, the data presented here suggest that partial inhibition of this checkpoint in tumor cells could result in acquisition of taxane resistance, while cells with more complete inhibition would be lost by apoptosis. Taxane treatment may result in selection of a population of cells with checkpoint function that has been partially attenuated but is still sufficient to support long-term growth and survival.

Ceramide Metabolism and Multidrug Resistance

Multidrug resistance mechanisms have proved difficult to define and to target effectively. Agents targeting the most well-known pathway, the multidrug-resistant transporters that promote drug resistance to structurally unrelated cytotoxic agents, have proved disappointing in clinical trials (Nobili et al., 2006). This screen revealed a small number of unexpected proteins that, when knocked down, led to sensitization to multiple drugs, suggesting that they may be important mediators of multidrug resistance. COL4A3BP siRNA was the strongest hit in this category, sensitizing diverse cell types to paclitaxel, doxorubicin, cisplatin, and 5-FU. A closer systematic analysis of the regulators of ceramide metabolism revealed other enzymes that impact strongly on drug sensitivity, including β-glucosidase (GBA), the Gaucher's disease gene product, which on knockdown promotes resistance to paclitaxel in all cell lines tested. COL4A3BP binds to ceramide and transports it from its site of de novo synthesis in the endoplasmic reticulum to the Golgi apparatus, where it is metabolized to sphingomyelin (Hanada et al., 2003). Reduction in COL4A3BP expression would be expected to result in accumulation of ceramide in the endoplasmic reticulum and increased total cellular ceramide. By contrast, β-glucosidase, also known as cerebrosidase, catalyzes the conversion of glucosylceramide to ceramide, so reducing its level would tend to decrease cellular ceramide levels (Ogretmen and Hannun, 2004). Ceramide has long been associated with promotion of apoptosis (Obeid et al., 1993), although the mechanisms involved have proved complex (Pettus et al., 2002). Many chemotherapeutic agents promote ceramide accumulation in cells, either due to increased de novo synthesis or sphingomyelinase activity opening up the therapeutic potential of this pathway (Kolesnick, 2002; Reynolds et al., 2004). It is thus logical that targeting COL4A3BP or GBA should lead to increased or decreased sensitivity to these drugs, respectively.

Previously, the only well-described connection between a ceramide pathway enzyme and multidrug resistance has been for glucosylceramide synthase (GCS, gene name *UGCG*), which catalyzes the reverse reaction to GBA, synthesizing glucosylceramide from ceramide in the Golgi. Targeting GCS has been shown to increase the sensitivity of breast cancer cells, including ADR/RES drug-resistant cells, to anthracyclines and taxanes (Liu et al., 2001), although we also show here that ADR/RES cells overexpress COL4A3BP and are sensitized to paclitaxel when it is knocked down. GCS siRNA did score as a drug sensitizer in our screen, for cisplatin in HCT-116 cells and doxorubicin in A549 cells, but was markedly weaker overall than COL4A3BP siRNA. Our data suggest that COL4A3BP would be likely to make a better therapeutic target for the reversal of multidrug resistance than GCS.

Akt activation is known to be suppressed by elevated ceramide levels, possibly in part due to the ability of ceramide to activate the phosphatase PP2A and in part due to inhibition of the PIP3-binding ability of the PH domain of Akt, perhaps due to direct phosphorylation by PKCζ (Powell et al., 2003; Stratford et al., 2001, 2004). Targeting *COL4A3BP* leads to decreased Akt activation state after paclitaxel treatment, while targeting *GBA* has the opposite effect. Accumulation of ceramide in the ER, while physically distant from the site of Akt activation at the plasma membrane, is able to inhibit Akt PH domain translocation.

It is possible that prolonged mitotic arrest is responsible for ceramide elevation by paclitaxel and that any inhibition

of this arrest would suppress ceramide generation and Akt suppression, thereby also promoting cell survival. While this could account for the effect of targeting mitotic checkpoint proteins on ceramide and phospho-Akt levels, it is less clear why targeting a ceramide-generating enzyme should affect the mitotic checkpoint, as is the case for GBA. It is possible that this could be due to decreased ceramide levels leading to elevated Akt activity at the mitotic checkpoint; activated Akt has been reported to overcome other cell-cycle checkpoints, such as a DNA-damage-induced G2/M checkpoint (Kandel et al., 2002) and also G1/S arrest, via phosphorylation of $p21^{Cip1/WAF1}$ and $p27^{KIP1}$ (Shin et al., 2002; Zhou et al., 2001).

The RNA interference approach taken here directly screens for single targets whose inhibition might reverse chemotherapeutic drug resistance in tumors: COL4A3BP represents one such candidate that clearly merits further investigation. It also identifies individual genes that when ablated promote drug resistance, such as various mitotic checkpoint regulators in the case of paclitaxel. Whether or not these have prognostic value, either alone or in combination, in predicting the response of tumors to chemotherapy, and how they compare with response signatures determined by gene expression profiling, will be the subject of further investigation.

EXPERIMENTAL PROCEDURES

Screen Set-Up

The Kinome (779 siRNAs) and Ceramidome libraries (50 siRNAs) were supplied by Dharmacon as SMARTpool collections. As negative control we used si*CONTROL* Non-Targeting siRNA pool (scrambled). HCT-116, A549, and MDA-MB-231 cells were transfected 24 hr after being plated on 96-well plates (Packard) with 70 nM siRNA using Oligofectamine transfection reagent (Invitrogen). After 48 hr, the appropriate cytotoxic drug was added: 58 nM paclitaxel (Sigma; HCT-116 and A549 cells) and 250 nM for MDA-MB-231, 50 μM 5-fluorouracil (5-FU, Calbiochem), 1 μM doxorubicin (Calbiochem), and 12.5 μM cisplatin (Sigma). Forty-eight hours later, the CellTiter-Glo Luminescent Cell Viability Assay (Promega) was performed.

Data Analysis: Derivation of Drug Sensitivity and Antagonism

In order to establish the influence of siRNA-induced knockdown of gene expression on drug sensitivity, the individual effects of drug and siRNAs on viability were taken into account. The viability effect of siRNA without drug compared to scrambled siRNA control was designated Rc/Cc. The effect of the drugs on viability of control-transfected cells was designated Cd/Cc. This enabled a calculation of the Expected combined effect of siRNA and drug on cell viability: Rc/Cc*Cd/Cc. The Observed combined effects of drug and siRNA on cell viability compared to untreated scrambled control transfected cells was designated Rd/Cc. Therefore, an index of antagonism or sensitivity (SI) for each siRNA was calculated by subtracting the Observed combined effect of drug and siRNA (Rd/Cc) from the Expected total viability effect: SI = (Rc/Cc*Cd/Cc) − (Rd/Cc). In order for the SI to usefully predict antagonism or sensitivity, an additional criteria that Rd/Cd > 1.05 (for antagonistic siRNAs) and Rd/Cd < 0.95 (for sensitizing siRNAs) was employed for hit selection. Further information on data analysis and statistical considerations can be found in the Supplemental Data.

Determination of Mitotic Index and Polyploidy

Cells were fixed with 70% ethanol and incubated with 6 μg/ml anti-MPM-2 antibody (Upstate) diluted in PBS/0.2% BSA for 1 hr. Cells were then washed and incubated with Alexa Fluor 488 conjugated antibody (Invitrogen) diluted in PBS containing 50 μg/ml RNaseA and 50 μg/ml propidium iodide and analyzed on a LSRII (Becton Dickinson). Cell doublets and debris were excluded from analysis on the basis of their pulse height and area, and at least 30,000 events were recorded.

CTCR-OV01 Clinical Trial and Consent Procedures

Ovarian cancer samples were obtained from the CTCR-OV01 study (http://pfsearch.ukcrn.org.uk/StudyDetail.aspx?TopicID=1&StudyID=1206). Patients with histologically confirmed advanced (stages III and IV) epithelial ovarian cancer with a WHO performance status of 0 or 1 were eligible to participate. Exclusion criteria were (1) nonepithelial ovarian tumors, (2) patients who had received prior chemotherapy or radiotherapy, and (3) patients who were not fit to receive paclitaxel treatment. Samples were collected immediately prior to chemotherapy and then 3 weeks postchemotherapy at debulking surgery from metastatic deposits in the abdomen. The study was approved by the Cambridge Local Research Ethics Committee (LREC). All patients gave written informed consent prior to participation.

Further description of experimental procedures can be found in the Supplemental Data.

Supplemental Data

The Supplemental Data include Supplemental Experimental Procedures, two supplemental tables, and four supplemental figures and can be found with this article online at http://www.cancercell.org/cgi/content/full/11/6/498/DC1/.

ACKNOWLEDGMENTS

We would like to thank C. Sachse and CENIX BioScience, GmbH, for their technical support; K. Hanada for LY-A cells; and Q. Bose, R. Gadelrab, and Dharmacon Inc. for technical assistance. We are grateful to K. Allen and D. Davies for flow cytometry expertise and to Thomas J. Hardcastle for bioinformatic analysis of the CTCR-OV01 data set. We are also grateful to A. Walther, A. Schulze, A. Venkitaraman, and D. Hancock for helpful discussions. This work was funded by Cancer Research UK.

Received: November 3, 2006
Revised: January 31, 2007
Accepted: April 2, 2007
Published: June 11, 2007

REFERENCES

Alaoui-Jamali, M.A., Dupre, I., and Qiang, H. (2004). Prediction of drug sensitivity and drug resistance in cancer by transcriptional and proteomic profiling. Drug Resist. Updat. *7*, 245–255.

Bettencourt-Dias, M., Giet, R., Sinka, R., Mazumdar, A., Lock, W.G., Balloux, F., Zafiropoulos, P.J., Yamaguchi, S., Winter, S., Carthew, R.W., et al. (2004). Genome-wide survey of protein kinases required for cell cycle progression. Nature *432*, 980–987.

Blagosklonny, M.V. (2006). Prolonged mitosis versus tetraploid checkpoint: how p53 measures the duration of mitosis. Cell Cycle *5*, 971–975.

Cahill, D.P., Lengauer, C., Yu, J., Riggins, G.J., Willson, J.K., Markowitz, S.D., Kinzler, K.W., and Vogelstein, B. (1998). Mutations of mitotic checkpoint genes in human cancers. Nature *392*, 300–303.

Carter, S.L., Eklund, A.C., Kohane, I.S., Harris, L.N., and Szallasi, Z. (2006). A signature of chromosomal instability inferred from gene expression profiles predicts clinical outcome in multiple human cancers. Nat. Genet. *38*, 1043–1048.

Chang, J.C., Wooten, E.C., Tsimelzon, A., Hilsenbeck, S.G., Gutierrez, M.C., Elledge, R., Mohsin, S., Osborne, C.K., Chamness, G.C., Allred, D.C., and O'Connell, P. (2003). Gene expression profiling for the prediction of therapeutic response to docetaxel in patients with breast cancer. Lancet *362*, 362–369.

de las Alas, M.M., Christen, R.D., Gately, D.P., Weiner, D.E., Benbatoul, K., Kirmani, S., D'Agostino, H.R., Plaxe, S.C., Darrah, D., McClay, E.F., et al. (2000). Increase in tumor GADD153 mRNA level following treatment correlates with response to paclitaxel. Cancer Chemother. Pharmacol. *45*, 381–388.

Eggert, U.S., Kiger, A.A., Richter, C., Perlman, Z.E., Perrimon, N., Mitchison, T.J., and Field, C.M. (2004). Parallel chemical genetic and genome-wide RNAi screens identify cytokinesis inhibitors and targets. PLoS Biol. *2*, e379. 10.1371/journal.pbio.0020379.

Ein-Dor, L., Zuk, O., and Domany, E. (2006). Thousands of samples are needed to generate a robust gene list for predicting outcome in cancer. Proc. Natl. Acad. Sci. USA *103*, 5923–5928.

Gouaze, V., Liu, Y.Y., Prickett, C.S., Yu, J.Y., Giuliano, A.E., and Cabot, M.C. (2005). Glucosylceramide synthase blockade down-regulates P-glycoprotein and resensitizes multidrug-resistant breast cancer cells to anticancer drugs. Cancer Res. *65*, 3861–3867.

Hanada, K., Kumagai, K., Yasuda, S., Miura, Y., Kawano, M., Fukasawa, M., and Nishijima, M. (2003). Molecular machinery for non-vesicular trafficking of ceramide. Nature *426*, 803–809.

Jin, J., and Woodgett, J.R. (2005). Chronic activation of protein kinase Bbeta/Akt2 leads to multinucleation and cell fusion in human epithelial kidney cells: events associated with tumorigenesis. Oncogene *24*, 5459–5470.

Kandel, E.S., Skeen, J., Majewski, N., Di Cristofano, A., Pandolfi, P.P., Feliciano, C.S., Gartel, A., and Hay, N. (2002). Activation of Akt/protein kinase B overcomes a G(2)/m cell cycle checkpoint induced by DNA damage. Mol. Cell. Biol. *22*, 7831–7841.

Kolesnick, R. (2002). The therapeutic potential of modulating the ceramide/sphingomyelin pathway. J. Clin. Invest. *110*, 3–8.

Kops, G.J., Foltz, D.R., and Cleveland, D.W. (2004). Lethality to human cancer cells through massive chromosome loss by inhibition of the mitotic checkpoint. Proc. Natl. Acad. Sci. USA *101*, 8699–8704.

Kumagai, K., Yasuda, S., Okemoto, K., Nishijima, M., Kobayashi, S., and Hanada, K. (2005). CERT mediates intermembrane transfer of various molecular species of ceramides. J. Biol. Chem. *280*, 6488–6495.

Le, X.F., Pruefer, F., and Bast, R.C., Jr. (2005). HER2-targeting antibodies modulate the cyclin-dependent kinase inhibitor p27(Kip1) via multiple signaling pathways. Cell Cycle *4*, 87–95.

Liu, Y.Y., Han, T.Y., Giuliano, A.E., and Cabot, M.C. (2001). Ceramide glycosylation potentiates cellular multidrug resistance. FASEB J. *15*, 719–730.

Longley, D.B., and Johnston, P.G. (2005). Molecular mechanisms of drug resistance. J. Pathol. *205*, 275–292.

Lonning, P.E., Sorlie, T., and Borresen-Dale, A.L. (2005). Genomics in breast cancer-therapeutic implications. Nat. Clin. Pract. Oncol. *2*, 26–33.

MacKeigan, J.P., Murphy, L.O., and Blenis, J. (2005). Sensitized RNAi screen of human kinases and phosphatases identifies new regulators of apoptosis and chemoresistance. Nat. Cell Biol. *7*, 591–600.

Moffat, J., Grueneberg, D.A., Yang, X., Kim, S.Y., Kloepfer, A.M., Hinkle, G., Piqani, B., Eisenhaure, T.M., Luo, B., Grenier, J.K., et al. (2006). A lentiviral RNAi library for human and mouse genes applied to an arrayed viral high-content screen. Cell *124*, 1283–1298.

Nobili, S., Landini, I., Giglioni, B., and Mini, E. (2006). Pharmacological strategies for overcoming multidrug resistance. Curr. Drug Targets *7*, 861–879.

Obeid, L.M., Linardic, C.M., Karolak, L.A., and Hannun, Y.A. (1993). Programmed cell death induced by ceramide. Science *259*, 1769–1771.

Ogretmen, B., and Hannun, Y.A. (2004). Biologically active sphingolipids in cancer pathogenesis and treatment. Nat. Rev. Cancer *4*, 604–616.

Pettus, B.J., Chalfant, C.E., and Hannun, Y.A. (2002). Ceramide in apoptosis: an overview and current perspectives. Biochim. Biophys. Acta *1585*, 114–125.

Potti, A., Dressman, H.K., Bild, A., Riedel, R.F., Chan, G., Sayer, R., Cragun, J., Cottrill, H., Kelley, M.J., Petersen, R., et al. (2006). Genomic signatures to guide the use of chemotherapeutics. Nat. Med. *12*, 1294–1300.

Powell, D.J., Hajduch, E., Kular, G., and Hundal, H.S. (2003). Ceramide disables 3-phosphoinositide binding to the pleckstrin homology domain of protein kinase B (PKB)/Akt by a PKCzeta-dependent mechanism. Mol. Cell. Biol. *23*, 7794–7808.

Reynolds, C.P., Maurer, B.J., and Kolesnick, R.N. (2004). Ceramide synthesis and metabolism as a target for cancer therapy. Cancer Lett. *206*, 169–180.

Roberts, J.R., Allison, D.C., Donehower, R.C., and Rowinsky, E.K. (1990). Development of polyploidization in taxol-resistant human leukemia cells in vitro. Cancer Res. *50*, 710–716.

Roschke, A.V., Tonon, G., Gehlhaus, K.S., McTyre, N., Bussey, K.J., Lababidi, S., Scudiero, D.A., Weinstein, J.N., and Kirsch, I.R. (2003). Karyotypic complexity of the NCI-60 drug-screening panel. Cancer Res. *63*, 8634–8647.

Shi, Q., and King, R.W. (2005). Chromosome nondisjunction yields tetraploid rather than aneuploid cells in human cell lines. Nature *437*, 1038–1042.

Shin, H.J., Baek, K.H., Jeon, A.H., Park, M.T., Lee, S.J., Kang, C.M., Lee, H.S., Yoo, S.H., Chung, D.H., Sung, Y.C., et al. (2003). Dual roles of human BubR1, a mitotic checkpoint kinase, in the monitoring of chromosomal instability. Cancer Cell *4*, 483–497.

Shin, I., Yakes, F.M., Rojo, F., Shin, N.Y., Bakin, A.V., Baselga, J., and Arteaga, C.L. (2002). PKB/Akt mediates cell-cycle progression by phosphorylation of p27(Kip1) at threonine 157 and modulation of its cellular localisation. Nat. Med. *8*, 1145–1152.

Slamon, D.J., Leyland-Jones, B., Shak, S., Fuchs, H., Paton, V., Bajamonde, A., Fleming, T., Eiermann, W., Wolter, J., Pegram, M., et al. (2001). Use of chemotherapy plus a monoclonal antibody against HER2 for metastatic breast cancer that overexpresses HER2. N. Engl. J. Med. *344*, 783–792.

Stratford, S., DeWald, D.B., and Summers, S.A. (2001). Ceramide dissociates 3′-phosphoinositide production from pleckstrin homology domain translocation. Biochem. J. *354*, 359–368.

Stratford, S., Hoehn, K.L., Liu, F., and Summers, S.A. (2004). Regulation of insulin action by ceramide: dual mechanisms linking ceramide accumulation to the inhibition of Akt/protein kinase B. J. Biol. Chem. *279*, 36608–36615.

Vogel, C., Kienitz, A., Hofmann, I., and Bastians, H. (2004). Crosstalk of the mitotic spindle assembly checkpoint with p53 to prevent polyploidy. Oncogene *23*, 6845–6853.

Watton, S.J., and Downward, J. (1999). Akt/PKB localisation and 3′ phosphoinositide generation at sites of epithelial cell-matrix and cell-cell interaction. Curr. Biol. *9*, 433–436.

Whitfield, M.L., Sherlock, G., Saldanha, A.J., Murray, J.I., Ball, C.A., Alexander, K.E., Matese, J.C., Perou, C.M., Hurt, M.M., Brown, P.O., and Botstein, D. (2002). Identification of genes periodically expressed in the human cell cycle and their expression in tumors. Mol. Biol. Cell *13*, 1977–2000.

Zhou, B.P., Liao, Y., Xia, W., Spohn, B., Lee, M.H., and Hung, M.C. (2001). Cytoplasmic localization of p21Cip1/WAF1 by Akt-induced phosphorylation in HER2/neu-overexpressing cells. Nat. Cell Biol. *3*, 245–252.